Three-nucleon potential effects in spin observables of elastic deuteron-proton scattering

Amir-Ahmadi, Hamid Reza

2. Theoretical background

Scattering is a mean to probe matter. The first particle scattering experiment, done by Rutherford, taught us that matter in an atom is not continuous, but is made of a small and dense core, the atomic nucleus, surrounded by an almost empty space (electron cloud). Scattering experiments are essential to examine and test our ideas about the constituents of matter and their interactions. Indeed, nuclear and particle physics could not have developed without scattering experiments.

Scattering experiments are used also to study the forces. One of these forces is the nuclear force which has not been derived from first principles (QCD) so far, but the valuable scattering data have enabled us to build up a potential which explains the nuclear phenomena. As it was discussed already in the introduction, the NN potential (NNP) is well studied using about 4300 experimental data points of NN scattering up to 350 MeV. There exists a sophisticated Partial-Wave Analysis (PWA), as well as five high-quality NNPs fitted to this data-base with a $\chi^2 \simeq 1$. These NNPs can describe the observables of two-nucleon systems very well.

To describe the observables of three- or many-nucleon systems, a NNP can be used; however, the results are not satisfactory. There are some effects which one may consider in order to account for the discrepancy between experimental results and theoretical calculations such as relativistic effect. Of course, this effect cannot resolve the problem in all experiments, e.g. very low-energy scattering. Another possibility is to add more potential terms to the NNP. In fact, the free parameters of the NNPs are fixed by the two nucleon scattering data, and as such they all reproduce only "on-shell" physics. In other words, the NNPs have the same on-shell properties but a different and arbitrary "off-shell" behavior. One notes that any of the off-shell effects included in any of these models cannot be examined experimentally. As already discussed in the previous chapter, in the three- or many-nucleon systems, it is important that the off-shell effects are properly handled. To resolve the discrepancies between data and theoretical calculations for three-nucleon systems, adding more potential terms such as a three-nucleon potential (3NP) is proposed. There are several 3NP models which have been developed by different groups. Any of the 3NP models can be added to one of the high-quality NNPs of interest.

The many-nucleon potential is still underdeveloped. Therefore, a three-nucleon (3N) system is a good start for this study. However, within chiral perturbation theory, it can be shown that the size of the 3NP is much smaller than the 2NP, the 4NP is much smaller than the 3NP, and so on. It is, therefore, a good assumption

that including the correct 2NP and 3NP in the calculations of many-body systems should be sufficient. Unfortunately, in contrast to two-nucleon systems, there is no good data-base for the three-nucleon system. A data-base for three-nucleon scattering could be used to examine the existing 3NPs. Also, one could perform a PWA of the three-nucleon system where the free parameters could be fitted using such data. A phase shift analysis below the breakup threshold has been already performed in Ref. [26].

In this chapter, the scattering formalism for two- and three-nucleon scattering will be reviewed. The general aspects of the NNPs and 3NPs will be introduced and at the end the observables which will be measured by this experiment are derived.

2.1 Scattering formalism

In this section, first the scattering theory in quantum mechanics will be reviewed and later it will be extended to the case of the three-body system. The derivations and notations in this section are mainly taken from Refs. [27, 28, 29].

2.1.1 Scattering formalism in quantum mechanics

In the framework of non-relativistic quantum mechanics, the state and evolution of a system is given by the Schrödinger equation:

$$i\hbar\frac{\partial}{\partial t}|\psi\rangle = H|\psi\rangle \quad \text{time-dependent} \tag{2.1}$$

and

$$H|\psi\rangle = E|\psi\rangle \quad \text{time-independent} \tag{2.2}$$

where the Hamiltonian is given by:

$$H = -\sum_i \frac{\hbar^2}{2m_i}\nabla_i^2 + V, \tag{2.3}$$

where i runs from 1 to the number of particles involved. The time evolution of the states is obtained from Eq. 2.1 as $|\psi(t)\rangle = \exp^{-iHt/\hbar}|\psi\rangle$, where $|\psi\rangle$ is the time-independent state. In a scattering problem, a beam of free particles comes close to a position where the particles interact with a potential V. Therefore, in the absence of any potential, $H = H_0 = -\sum_i \frac{\hbar^2}{2m_i}\nabla_i^2$, the scattering state $|\psi(t \to -\infty)\rangle$ must be equal to a free state of $|\phi(t)\rangle = \exp^{-iH_0t/\hbar}|\phi\rangle$ with the same energy

$$\lim_{t\to-\infty} \| \exp^{-iHt/\hbar}|\psi\rangle - \exp^{-iH_0t/\hbar}|\phi\rangle\| = 0. \tag{2.4}$$

It can be shown [28] that the relation between the scattering state and the free-particle state is

$$|\psi^{\pm}\rangle = \lim_{\epsilon \to 0} i\epsilon \frac{1}{E - H \pm i\epsilon} |\phi\rangle. \tag{2.5}$$

One can define $G_{\pm} = \frac{1}{E-H\pm i\epsilon}$ as the resolvent or the Green's function for the Helmholtz equation

$$(\nabla^2 + k^2) G_{\pm}(\vec{x}, \vec{x}') = \delta(\vec{x} - \vec{x}'). \tag{2.6}$$

Using operator algebra, the Green's function can be decomposed depending on the problem of interest. For instance, in case of two interacting particles with potential V, one can write

$$\frac{1}{E - H \pm i\epsilon} = \frac{1}{E - H_0 \pm i\epsilon} + \frac{1}{E - H_0 \pm i\epsilon} V \frac{1}{E - H \pm i\epsilon} = G_0 + G_0 V G \tag{2.7}$$

where $G_0 = (E - H_0 \pm i\epsilon)^{-1}$ is sometimes called the free-particle propagator. By inserting Eq. 2.7 into Eq. 2.5 and using the fact that $i\epsilon G_0 |\phi\rangle = |\phi\rangle$, we obtain the *Lippmann-Schwinger Equation* (LSE)

$$|\psi^{\pm}\rangle = |\phi\rangle + G_0 V |\psi^{\pm}\rangle. \tag{2.8}$$

Note that at large distances, the wave function $\langle \vec{x} | \psi^{\pm} \rangle$ is written as the sum of the incident wave $\langle \vec{x} | \phi \rangle$ and an outgoing (incoming) spherical wave corresponding to the positive (negative) solution. The homogeneous LSE, $|\psi\rangle = G_0 V |\psi\rangle$, has no solution for the positive energy $E > 0$. Because, if a solution exists it must fulfill the Schrödinger equation and a solution of the Schrödinger equation conserves probability. The homogeneous solution, however, does not contain the incident wave and, thus, cannot conserve the probability. Therefore, the inhomogeneous equation has a unique solution. This is only true for the two-body system. For the three-body system, the LSE does not have a unique solution. To obtain a unique solution for the 3N system, supplementary conditions are necessary [29]. This will be discussed in the next section.

In a scattering problem, the most interesting subject is the transition of the initial state to the scattering state by means of a potential. The transition operator, t, is defined with

$$V |\psi^{+}\rangle \equiv t |\phi\rangle. \tag{2.9}$$

Multiplying the LSE by V from the left results in

$$t = V + V G_0 t. \tag{2.10}$$

The cross section is directly related to the *t-matrix* which is the matrix element of the transition operator in momentum space via

$$\frac{d\sigma}{d\Omega} \propto |\langle p'|t(E+i\epsilon)|p\rangle|^2, \tag{2.11}$$

where $E = \frac{p'^2}{2\mu} = \frac{p^2}{2\mu}$ and μ is the reduced mass. Of course, if the energy is not conserved (off-shell particles) then $E \neq \frac{p'^2}{2\mu} \neq \frac{p^2}{2\mu}$. However, the observables for two-nucleon scattering are determined by on-shell t-matrix. The t-operator and therefore the t-matrix can be evaluated iteratively

$$t = V + VG_0V + VG_0VG_0V + VG_0VG_0VG_0V + ... \tag{2.12}$$

This can be shown diagrammatically as

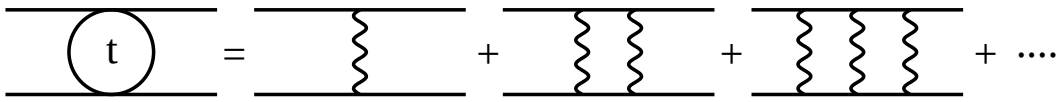

where all irreducible diagrams are included in the kernel, the potential V:

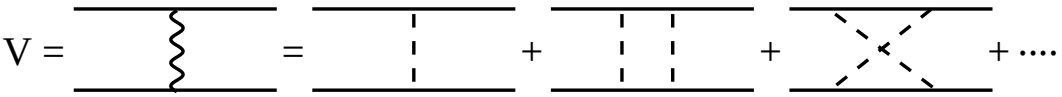

The dashed lines show pions.

2.1.2 Three-nucleon scattering

The Hamiltonian for the 3N system is written as

$$H = -\sum_{i=1}^{3} \frac{\hbar^2}{2m_i}\nabla_i^2 + \sum_{i>j=1}^{3} v_{ij} + \sum_{i>j>k=1}^{3} v_{ijk} \tag{2.13}$$

where v_{ij} is the NNP and v_{ijk} is the three-nucleon potential (3NP) with a cyclic permutation of ijk. From experimental and theoretical investigations, we already know that the 3N potential is smaller than the NNP in magnitude. If we just consider the NNP, the results of the theoretical calculations for most observables are close to the measurements. Let us, then, start with the formalism of treating the three-body system with only the NNP and later add the 3NP to it. Consider three particles with mass m_i and momentum $\vec{k}_i$ conjugate to $\vec{x}_i$. We need a coordinate system in which the center-of-mass motion is separated out. The Faddeev choice of coordinates in

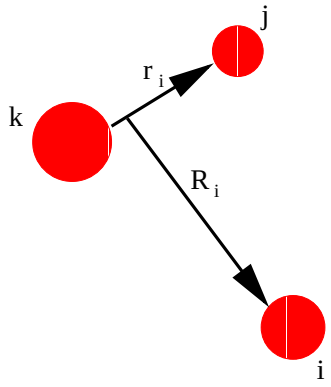

Figure 2.1: The Jacobi coordinate system. The particles j and k are two-nucleon subsystem and i is a spectator.

which he could nicely decompose the Schrödinger equation for the 3N system was the Jacobi coordinate system. There are three possibilities to have a two-nucleon subsystem in a three-nucleon system. Suppose particles j and k are the two-nucleon subsystem and particle i is the third particle $(i, j, k = 1, 2, 3)$; as shown in Fig. 2.1:

$$\begin{aligned} \vec{r}_i &\equiv \vec{x}_j - \vec{x}_k, \\ \vec{R}_i &\equiv \vec{x}_i - \frac{m_j\vec{x}_j + m_k\vec{x}_k}{m_j + m_k}, \\ \vec{\eta} &\equiv \frac{m_i\vec{x}_i + m_j\vec{x}_j + m_k\vec{x}_k}{m_i + m_j + m_k}. \end{aligned} \tag{2.14}$$

The conjugate momenta for the new coordinates are

$$\begin{aligned} \vec{p}_i &= \frac{m_j\vec{k}_k - m_k\vec{k}_j}{m_j + m_k}, \\ \vec{q}_i &= \frac{(m_j + m_k)\vec{k}_i - m_i(\vec{k}_j + \vec{k}_k)}{m_i + m_j + m_k}, \\ \vec{K} &= \vec{k}_i + \vec{k}_j + \vec{k}_k. \end{aligned} \tag{2.15}$$

The momenta, $\vec{p}_i$, which is the conjugate of $\vec{r}_i$, is the relative momentum of particles j and k; $\vec{q}_i$ which is the conjugate momentum of $\vec{R}_i$, is the relative momentum of particle i with respect to c.m. of $j - k$ particles; and $\vec{K}$ which is the conjugate momentum of $\vec{\eta}$, is the total momentum of the three particles. Now, we can write the Hamiltonian with only the NN interaction in the new coordinate system as

($\alpha = 1, 2$ or 3)

$$H' = \frac{K^2}{2(m_1+m_2+m_3)} + \frac{p_\alpha^2}{2\mu_\alpha} + \frac{q_\alpha^2}{2M_\alpha} + \sum_{i=1}^{3} V_i, \tag{2.16}$$

where $V_i \equiv V_{jk}(|\vec{x}_j - \vec{x}_k|)$, $\frac{1}{\mu_i} = \frac{1}{m_j} + \frac{1}{m_k}$ and $\frac{1}{M_i} = \frac{1}{m_i} + \frac{1}{m_j+m_k}$. The total c.m. motion is not important for this discussion and can be left out. The configuration of a bound pair and a free particle is, then, described by

$$\langle \vec{r}_i, \vec{R}_i | \Phi_i \rangle = \Phi_i(\vec{r}_i, \vec{R}_i) = \phi_i(\vec{r}_i) e^{i\vec{q}_i \cdot \vec{R}_i}, \tag{2.17}$$

which is the solution of

$$H_i |\Phi_i\rangle = E_i |\Phi_i\rangle, \tag{2.18}$$

where

$$H_i = \frac{p_i^2}{2\mu_i} + \frac{q_i^2}{2M_i} + V_i \tag{2.19}$$

is called the *channel Hamiltonian* and $E_i = (q_i^2/2M_i) + e_i$ is the total energy E in the c.m. frame and e_i is the binding energy for $\phi_i(r_i)$. Obviously, there are three configurations in each of which two of the particles are interacting and the third one is spectator. The configuration is described with the Schrödinger equation

$$h|\psi_i^+\rangle \equiv (H_i + V_j + V_k)|\psi_i^+\rangle = E|\psi_i^+\rangle. \tag{2.20}$$

The solution of this equation is

$$|\psi_i^+\rangle = \lim_{\epsilon \to 0} i\epsilon \frac{1}{E - h + i\epsilon} |\Phi_i\rangle. \tag{2.21}$$

We can again decompose the Green's function as

$$\frac{1}{E - h \pm i\epsilon} = \frac{1}{E - H_i \pm i\epsilon} + \frac{1}{E - H_i \pm i\epsilon}(V_j + V_k)\frac{1}{E - h \pm i\epsilon}. \tag{2.22}$$

Inserting Eq. 2.22 into Eq. 2.21 gives the LSE

$$|\psi_i^+\rangle = |\Phi_i\rangle + G_i(V_j + V_k)|\psi_i^+\rangle, \tag{2.23}$$

where $G_i = \lim_{\epsilon \to 0}(E - H_i \pm i\epsilon)^{-1}$.

It can be shown that this LSE does not have a unique solution for a three- or more-body system as opposed to the two-body system [30]. The $|\psi_j^+\rangle$ and $|\psi_k^+\rangle$ with $j, k \neq i$ are also solutions of Eq. 2.23. More boundary conditions are needed in order

to get a unique solution. Glöckle has shown that $|\psi_i^+\rangle$ satisfies the following two homogeneous equations as well [29]:

$$|\psi_i^+\rangle = G_j(V_i + V_k)|\psi_i^+\rangle, \tag{2.24}$$
$$|\psi_i^+\rangle = G_k(V_j + V_i)|\psi_i^+\rangle. \tag{2.25}$$

These two homogeneous equations and the LSE (Eq. 2.23) are called *Lippmann-Schwinger triad* and can be written in one equation as

$$|\psi_i^+\rangle = \delta_{il}|\Phi_i\rangle + G_l(V_j + V_k)|\psi_i^+\rangle, \tag{2.26}$$

where the permutation of ljk is cyclic and $l = i, j$ or k. It can also be shown that the solution of the triad must be a solution of the Schrödinger equation with $E > 0$; it is unique and corresponds to an outgoing spherical wave.

Similar to NN scattering, one can define a transition operator. Consider that we have now the three equations of a triad. As in the NN case, Eq. 2.10, we can write

$$T = V + VG_0T. \tag{2.27}$$

This T-operator has the same singularity problem as Eq. 2.23 since they have the same kernel. To solve the problem, Faddeev splits Eq. 2.27 into three equations [31]. Because $V = V_1 + V_2 + V_3$, one can write

$$\begin{aligned} T &= (V_1 + V_2 + V_3) + (V_1 + V_2 + V_3)G_0T \\ &= \sum_{i=1}^{3}(V_i + V_iG_0T) = \sum_{i=1}^{3} T_i, \end{aligned} \tag{2.28}$$

where

$$T_i \equiv V_i + V_iG_0T. \tag{2.29}$$

Let us arrange Eq. 2.29 as

$$T_i - V_iG_0T_i = V_i + V_iG_0(T_j + T_k), \quad \{i \neq j \neq k\} = \{1, 2 \text{ and } 3\}. \tag{2.30}$$

By defining $t_i \equiv (1 - V_iG_0)^{-1}V_i$ one can write Eq. 2.30 as

$$T_i = t_i + t_iG_0(T_j + T_k), \tag{2.31}$$

or in matrix form

$$\begin{pmatrix} T_1 \\ T_2 \\ T_3 \end{pmatrix} = \begin{pmatrix} t_1 \\ t_2 \\ t_3 \end{pmatrix} + \begin{pmatrix} 0 & t_1 & t_1 \\ t_2 & 0 & t_2 \\ t_3 & t_3 & 0 \end{pmatrix} G_0 \begin{pmatrix} T_1 \\ T_2 \\ T_3 \end{pmatrix}. \tag{2.32}$$

This is the Faddeev T-matrix. If we just compare t_i with Eq. 2.10, we will recognize it as a two-body T-matrix in three-body space. In contrast to the NN T-matrix, t_i contains off-shell information because of the energy shift of $E - q_i'^2/2M_i$ which is due to an extra term in the channel Hamiltonian. Having a set of coupled equations and terms like $t_i G_0 T_j$ implies an integration over all possible intermediate states $|p_i'' q_i''\rangle$ with

$$\frac{p_i^2}{2\mu_i} \neq \frac{p''^2_i}{2\mu_i} \neq E + i\epsilon - \frac{q''^2_i}{2M_i}. \tag{2.33}$$

Iteration of the Faddeev T-matrix, Eq. 2.32, describes the 3N scattering as a multiple NN scattering where the NN sub-system scattering can be on-shell or off-shell. The first iteration is

$$\begin{pmatrix} T_1 \\ T_2 \\ T_3 \end{pmatrix} = \begin{pmatrix} t_1 \\ t_2 \\ t_3 \end{pmatrix} + \begin{pmatrix} t_1 G_0 (t_2 + t_3) \\ t_2 G_0 (t_3 + t_1) \\ t_3 G_0 (t_1 + t_2) \end{pmatrix}$$

$$+ \begin{pmatrix} t_1 G_0 (t_2 + t_3) & t_1 G_0 t_3 & t_1 G_0 t_2 \\ t_2 G_0 t_3 & t_2 G_0 (t_3 + t_1) & t_2 G_0 t_1 \\ t_3 G_0 t_2 & t_3 G_0 t_1 & t_3 G_0 (t_1 + t_2) \end{pmatrix} G_0 \begin{pmatrix} T_1 \\ T_2 \\ T_3 \end{pmatrix}, \tag{2.34}$$

which consists of terms such as $t_1 G_0 t_3$ that can be represented diagrammatically as:

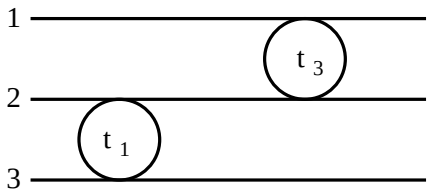

A Neumann series of the Faddeev equations, Eq. 2.34, for T_1 is shown in Fig. 2.2. In every NN scattering, only a pair of particles interact and the third particle is free. Then, the three particles propagate freely to the next NN scattering. The state of the third non-interacting particle does not change and this will be expressed mathematically by a δ-function:

$$\langle p_i q_i | t_i (E + i\epsilon) | p_i' q_i' \rangle = \delta(q_i - q_i') \langle p_i | t_i (E + i\epsilon - \frac{q_i'^2}{2M_i}) | p_i' \rangle. \tag{2.35}$$

Fortunately, this δ-function disappears when integrating over possible intermediate states. This is the advantage of the iteration.

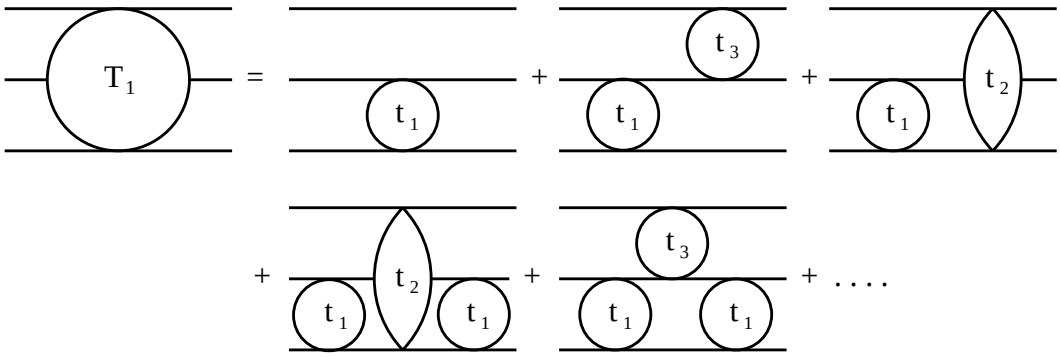

Figure 2.2: Diagrammatic representation of T_1.

Inclusion of the 3NP

The 3NP can be added to the pairwise part of potential of the 3N system [32, 33] which is already decomposed using the Jacobi coordinate system. Let us represent the 3NP by V_4. Equation 2.21 does not change except that now $h = H_0 + V_1 + V_2 + V_3 + V_4$. It seems natural to modify the integral kernels of Eq. 2.26 to

$$|\psi_i^+\rangle = \delta_{il}|\Phi_i\rangle + G_l V^l |\psi_i^+\rangle, \tag{2.36}$$

where $V^l = (V_j + V_k + V_4)$. Hereafter, all Roman indices take values 1,2,3 and number 4 is indicated specifically. Although this equation already determines the scattering state of $|\psi_i^+\rangle$ uniquely, one can still define an auxiliary equation:

$$|\psi_i^+\rangle = G_4(V_1 + V_2 + V_3)|\psi_i^+\rangle \tag{2.37}$$

where $G_4 \equiv \lim_{\epsilon\to 0}(E - H_0 - V_4 + i\epsilon)^{-1}$ satisfies the following Lippmann identity

$$\lim_{\epsilon\to 0} i\epsilon G_4(E + i\epsilon)|\phi_i\rangle = 0. \tag{2.38}$$

The inclusion of 3NP in the Faddeev equation for the T-operator, Eq. 2.27, can be achieved by splitting the T-operator into four parts rather than the three parts as was done in Eq. 2.29.

2.2 NN potentials

The phenomenological NNPs are based on the most general form for a potential which is restricted by symmetries [2]. The potential must be invariant under rotation, reflection and time reversal. The model-independent terms are written in the

configuration space as a sum of 6 terms, $V = \sum_{i=1}^{6} V_i P_i$, where

$$\begin{aligned} P_1 &= 1, \\ P_2 &= \vec{\sigma}_1 \cdot \vec{\sigma}_2, \\ P_3 &= S_{12} = 3(\vec{\sigma}_1 \cdot \hat{r})(\vec{\sigma}_2 \cdot \hat{r}) - \vec{\sigma}_1 \cdot \vec{\sigma}_2, \\ P_4 &= \vec{L} \cdot \vec{S}, \\ P_5 &= Q_{12} = \frac{1}{2}[(\vec{\sigma}_1 \cdot \vec{L})(\vec{\sigma}_2 \cdot \vec{L}) + (\vec{\sigma}_2 \cdot \vec{L})(\vec{\sigma}_1 \cdot \vec{L})], \\ P_6 &= (\vec{\sigma}_1 - \vec{\sigma}_2) \cdot \vec{L}. \end{aligned} \tag{2.39}$$

In general, V_i is a function of the distance between two nucleons, r, and the operators of linear and angular momentum p^2 and L^2 and, thus, generally independent of partial waves. These 6 terms are multiplied by isospin operators $\mathbf{1}$ or $\vec{\tau}_1 \cdot \vec{\tau}_2$. In the modern high-quality NNPs such as NijmI, NijmII and Reid93, up to $E_{lab} = 350$ MeV, V_i is also a function of S^2 and J^2 which results from the fact that each partial wave is parameterized separately. These new potentials have been fitted to about 4000 data points with $\chi^2/datum \simeq 1$. The best potential models up to 1980 and including the models of the 1980s had only $\chi^2/datum \simeq 2$ [2].

After discovery of heavy mesons in the 1960s, the NNPs were written as a sum of the potentials representing exchanged bosons. The long range part ($\gtrsim 2$ fm) of the potential is governed by the π-meson and is, therefore, called the One-Pion-Exchange Potential (OPEP). As Eq. 1.1 shows, at shorter distances, the attractive medium-range, a heavier meson such as the σ-meson or two π-mesons could be exchanged. The short-range ($\lesssim 1.4$ fm) repulsive part of the NNP needs a heavy vector boson such as the ω-meson or ρ-meson. The high-quality NNPs explain the long-range part of the potential by employing the OPEP together with the electromagnetic interaction, and the shorter range is normally treated phenomenologically.

The short-range repulsive part is short enough to be screened by a centrifugal barrier for the higher partial waves [34]. In other words, the partial waves with higher angular momenta do not need to be parameterized and only the partial-waves of low angular momenta, normally up to $J = 5$, are parameterized. For the partial waves of lower angular momenta, the short-range part is represented by an energy dependent square-well of range $r = b = 1.4$ fm. The depth of square-well is independent of r but energy dependent which is, therefore, different for each of the partial-waves. In general, the NNP is written as a sum of an electromagnetic part, an OPEP part and an intermediate- and short-range phenomenological part:

$$v(NN) = v_{EM}(NN) + v_{\pi}(NN) + v_I(NN) + v_S(NN). \tag{2.40}$$

The OPEP for pp scattering is given by

$$v_{\pi}(pp) = f_{\pi}^2 V(m_{\pi^0}), \tag{2.41}$$

and for np scattering it is

$$v_\pi(np) = -f_\pi^2 V(m_{\pi^0}) + (-)^{I+1} 2 f_\pi^2 V(m_{\pi^\pm}), \tag{2.42}$$

where I is the isospin and

$$V(m) = \left(\frac{m}{m_{\pi^\pm}}\right)^2 \frac{1}{3} mc^2 [V_S(r)\vec{\sigma}_i \cdot \vec{\sigma}_j + V_T(r) S_{ij}]. \tag{2.43}$$

$V_S(r)$ and $V_T(r)$ are the Yukawa and tensor functions:

$$\begin{aligned} V_S(r) &= \frac{e^{-\mu r}}{\mu r}, \\ V_T(r) &= \left(1 + \frac{3}{\mu r} + \frac{3}{(\mu r)^2}\right) \frac{e^{-\mu r}}{\mu r}, \end{aligned} \tag{2.44}$$

where $\mu = mc/\hbar$ [4] and $f_\pi^2 = 0.075$ is the pion-nucleon coupling constant [35]. A part of the intermediate-range attraction is often explained by σ-meson exchange for which the potential is given by

$$v_\sigma = g^2 [V_c(r) + V_{LS}(r) \vec{L} \cdot \vec{S}]. \tag{2.45}$$

There are several high-quality NNPs based on One-Boson-Exchange (OBE). They have been fitted to the world NN scattering data-set up to 350 MeV and they are all non-relativistic. However, they take the relativistic effects into account by using a relativistic momentum. I will briefly explain some of the aspects of the models which were used in predicting the observables of the present experiment.

The Nijmegen group has introduced NijmI, NijmII and Reid93 potential models and Partial-Wave Analysis PWA93 [2]. The PWA93 has 39 parameters and has been fitted to almost 4300 data points with $\chi^2/datum \simeq 0.99$. This can be compared to, for instance, Nijm93 which fits the NN data with $\chi^2/datum = 1.87$ and has only 15 parameters. The relativistic effects are estimated via the potential and by using the relativistic relation between the three-momentum and laboratory kinetic energy.

The newest Charge-Dependent (CD) Bonn potential which is the successor of the original Bonn potential is called CD-Bonn [3]. This high-quality potential fits 2932 pp scattering data points with $\chi^2/datum = 1.01$ and 3058 np scattering data points with $\chi^2/datum = 1.02$. It is based on meson exchange and all mesons with masses smaller than the nucleon mass are included. The group responsible for this potential has also studied Charge-Independence Breaking (CIB) and Charge-Symmetry Breaking (CSB), since the pp and nn interactions are different even after removing the electromagnetic interaction (CSB).

Another high-quality NNP is Argonne v_{18} (AV_{18}) [4]. This potential has 18 operators. Fourteen operators are charge-independent corresponding to an updated version of Argonne v_{14} [36]. Three charge-dependent operators have been added because of isospin-breaking aspect of the strong interaction and one charge-asymmetric operator to explain the difference in the pp and nn scattering lengths. AV_{18} has 40 parameters which have been adjusted via fitting the model to 4300 pp and np scattering data points from the Nijmegen data-base with $\chi^2/datum = 1.09$. The AV_{18} is also corrected for relativistic effects. Since the NN interaction depends on the relative momentum $\vec{p}_{ij} = (\vec{p}_i - \vec{p}_j)/2$ of the two nucleons and the total momentum $\vec{P}_{ij} = \vec{p}_i + \vec{p}_j$, one writes

$$v_{ij} = \tilde{v}_{ij} + \delta v(\vec{P}_{ij}), \tag{2.46}$$

where v_{ij} is the potential between particle i and j and $\tilde{v}_{ij}$ is the first-order not corrected potential; $\delta v(P_{ij} = 0) = 0$, and

$$\delta v(P_{ij}) = -\frac{P_{ij}^2}{8m^2}\tilde{v} + \frac{1}{8m^2}[\vec{P}_{ij} \cdot \vec{r}\vec{P}_{ij} \cdot \vec{\nabla}, \tilde{v}] + \frac{1}{8m^2}[(\vec{\sigma}_1 - \vec{\sigma}_2) \times \vec{P}_{ij} \cdot \vec{\nabla}, \tilde{v}]. \tag{2.47}$$

The *boost correction* of $\delta v(P_{ij})$ has a repulsive contribution in the binding energy of ^{3}H and ^{4}He [7].

In spite of the good performance of the high-quality NNPs, the potentials still have problems which need further attention. To transform the potentials written in momentum space to configuration space by means of Fourier transform, a form-factor is needed to handle the singularity at the origin [2]. This form-factor is not fixed by theory or experiment. Every model takes a form-factor that fits better to the data-set. One of the scalar mesons, the σ-meson, which in OBEPs is necessary to explain especially the medium-range attraction has not yet been definitely observed experimentally. The high-quality models, such as NijmI, have more parameters to be fitted to the data than the OBE models, such as Nijm93. Therefore, they necessarily depend on the choice of parameters, and this leaves still some freedom in the way they are parameterized. Comparing the NN phases for different NN models show deviations specially above 200 MeV [27]. These are some of the issues that leave room for more developments in the construction of NNPs.

2.3 Three-nucleon potential models

The first 3NP model was developed by Fujita and Miyazawa (FM) [11]. They described the 3N interaction by Two-Pion Exchange (TPE) and one intermediate Δ-isobar excitation, as illustrated in the right diagram in Fig 2.3. The main ingredient of TPE-models is the πN scattering amplitude such as T_3 in Fig 2.3 (left diagram).

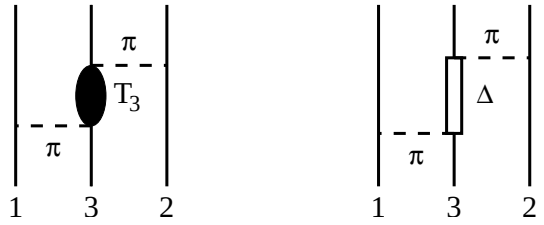

Figure 2.3: Left: the Feynman diagram for the TPE where T_3 represents πN scattering amplitude with all three nucleons involved. Right: A TPE with Δ-isobar excitation as one of the possibilities for T_3. This is used in FM model.

The models developed later included other possibilities for the T_3 scattering amplitude. The Tucson-Melbourne potential (TM) is an example of this, see Sec. 2.3.1. In the TM model, T_3 is the full pion-nucleon interaction except for a propagation of the pion which does not interact with the middle nucleon, because this is already included in the NNP.

Theoretical predictions for the observables of our interest were calculated by three groups. The Bochum-Cracow group used the modified-TM-model [37, 38] which is called TM′ or TM99 as 3NP. They added TM′ to the NN models, CD-Bonn, NijmI, NijmII and AV_{18}. They have also used the Urbana-IX [7] 3NP which is developed by the Argonne-Illinois group to be added to AV_{18}. The Hanover group has also calculated the observables for our H$(\vec{d},\vec{p})d$ reaction with the Δ-isobar treated dynamically [39], see Sec. 2.3.3. The third calculation was performed using Chiral Perturbation Theory (χPT) [40]. The χPT will be discussed in Sec. 2.3.4. The TM99 is described in some detail in the following section after which the other 3NP models are briefly discussed.

2.3.1 Tucson-Melbourne potential

The Tucson-Melbourne potential (TM) is a 3NP model of the TPE type [12]. TM includes the πN scattering amplitude in which the pions are off-mass-shell[1], i.e. $E_\pi^2 \neq p_\pi^2 + \mu^2$, where μ is the pion mass. In contrast to the FM model which considers only the p-wave Δ-isobar excitation, the TM model includes also other possibilities for the πN scattering amplitude, see Fig. 2.3. In general, the FM model or other models based on the Δ-isobar are a special case of TM models.

There are three geometrical configurations of three nucleons for which one of the three nucleons is in the middle; see Fig 2.3. The notation $V_4^{(3)}$ stands for a 3NP

[1] This is needed for the exchange of virtual space-like pions in a nuclear-force diagram.

where nucleon 3 is in the middle, so the full 3NP is

$$V_4 = \sum_{i=1}^{3} V_4^{(i)}. \tag{2.48}$$

Using this notation, the TM potential is [41]

$$\begin{aligned}\langle \vec{p_1'}\vec{p_2'}\vec{p_3'}|V_4^{(3)}|\vec{p_1}\vec{p_2}\vec{p_3}\rangle = (2\pi)^3\delta^3(\vec{p_1}+\vec{p_2}+\vec{p_3}-\vec{p_1'}-\vec{p_2'}-\vec{p_3'}) \\ \frac{(\vec{\sigma}_1\cdot\vec{Q})(\vec{\sigma}_2\cdot\vec{Q}')}{(Q^2+\mu^2)(Q'^2+\mu^2)}\frac{g_{\pi NN}^2}{4m_N^2}F_{\pi NN}^2(Q^2)F_{\pi NN}^2(Q'^2)[T_{\pi\mathrm{N}}^{\alpha\beta}\tau_1^\alpha\tau_2^\beta].\end{aligned} \tag{2.49}$$

The T-matrix for πN scattering is

$$T_{\pi\mathrm{N}}^{\alpha\beta} = \delta^{\alpha\beta}[a + b\vec{Q}\cdot\vec{Q}' + c(Q^2+Q'^2)] - d(\tau_3^\gamma\epsilon^{\alpha\beta\gamma}\vec{\sigma}_3\cdot\vec{Q}\times\vec{Q}'), \tag{2.50}$$

where α and β are the isospin labels of the initial and final states, $\vec{p_i}$ and $\vec{p_i'}$ are incoming and outgoing momenta of the nucleons, $\vec{Q} = \vec{p_1} - \vec{p_1'}$, $\vec{Q}' = \vec{p_2'} - \vec{p_2}$; see Fig. 2.4; $g_{\pi NN}$ is the pion-nucleon coupling constant; σ_i and τ_i are the spin and isospin operators, respectively. $F_{\pi NN}(Q^2)$ is the form-factor of the πNN vertex when the nucleons are on-the-mass-shell and the pion is off-the-mass-shell:

$$F_{\pi NN}(Q^2) = \frac{\Lambda^2-\mu^2}{\Lambda^2-Q^2}. \tag{2.51}$$

Here, Λ is the cut-off parameter which is fitted to data.

In Eq. 2.50, the πN scattering amplitude is parameterized. The parameters a, b, c and d are obtained by fitting the amplitude to the πN scattering data. In the TM model, the strength parameters are $a = 1.13/\mu$, $b = -2.58/\mu^3$, $c = 1.0/\mu^3$ and $d = -0.753/\mu^3$ and the corresponding term consists of several πN scattering diagrams [41]. For instance, the Δ contribution is included in the b-term.

The calculation of the triton binding energy including the TM potential yields an overbinding and a strong dependence on the πNN form-factor. The value of the cut-off parameter, Λ, is taken to reproduce the ^{3}H binding energy [42]. The potential was modified and developed further by adding other meson exchanges; e.g., $\pi-\rho$ and $\rho-\rho$ were added to the model to have more complete two-meson-exchange 3NP [37]. This TM model is sometimes referred to as TM93 [38].

The parameterization of the TM model was criticized later by Friar et al. [43], since it was not fully chirally symmetric; see Sec. 2.3.4. They obtained the TM 3NP by the chiral-perturbation-theory (χPT) approach and showed that the c-term is unnatural and must be dropped. The parameters obtained in this approach are

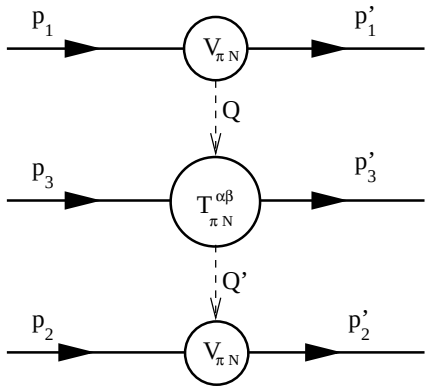

Figure 2.4: TPE diagram. Solid lines represent nucleons and dashed lines pions. $V_{\pi\mathrm{N}}$ is the πNN vertex and $T^{\alpha\beta}_{\pi\mathrm{N}}$ is the amplitude for πN scattering. The momentum of nucleons before and after scattering are shown by p_i and ${p'}_i$ and $Q = p_1 - {p'}_1$ and $Q' = {p'}_2 - p_2$ are the pion momenta.

different from those of TM model: $a' \propto -a$ and $c = 0$. This model is sometimes referred to as the *Texas model*.

The latest TM model was introduced by Coon and Han, taking into account all previous developments [38]. The c-term was decomposed into a 2π-exchange term, which can be added to a-term, and a short-range term. Therefore, in the latest model, which is named TM$'$, the parameters are a', b and d, where a' is related to the old parameters by $a' = a - 2\mu^2 c$.

2.3.2 Urbana-IX and Illinois potentials

After developing the NNP of Argonne v_{18} (AV_{18}), the Urbana-Argonne collaboration in Illinois introduced new phenomenological 3NPs, namely Urbana-IX (UIX) and Illinois1-5 [7]. These 3NPs together with the AV_{18} NN-potential have been developed to fix the binding energy of the first few light nuclei, as was shown in Fig. 1.1. The three-nucleon potentials developed by the Illinois group have the following general form:

$$V_{ijk} = A_{2\pi}^{SW} O_{ijk}^{2\pi,SW} + A_{2\pi}^{PW} O_{ijk}^{2\pi,PW} + A_{3\pi}^{\Delta R} O_{ijk}^{3\pi,\Delta R} + A_R O_{ijk}^{R}, \tag{2.52}$$

where the terms represent TPE due to s-wave and p-wave πN scattering, three-pion-exchange due to ring diagrams with one Δ in the intermediate states and a repulsive term respectively; see Fig. 2.5. $A_{2\pi}^{SW}, A_{2\pi}^{PW}, A_{3\pi}^{\Delta R}$ and A_R are the strengths of the terms. The UIX potential does not have the s-wave and the three-pion-exchange terms [7].

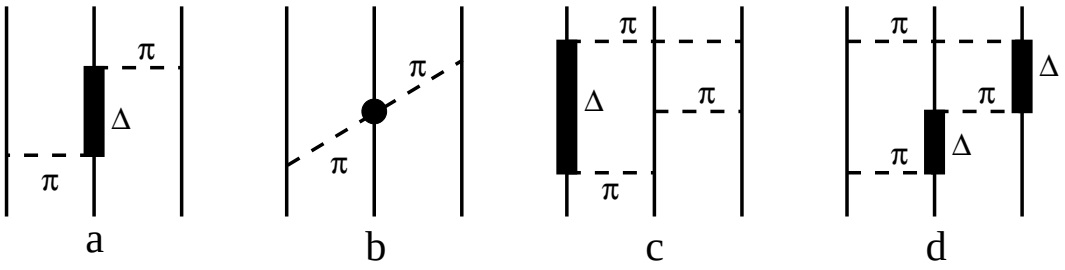

Figure 2.5: Feynman diagrams for 3NP of the Illinois group: a) the FM potential (TPE p-wave), b) TPE s-wave, c) and d) three-pion rings with one Δ at a time in intermediate states.

The spin-isospin and spatial dependence of the terms was obtained from theoretical models but the strength of the terms was fixed by fitting to the binding energies of light nuclei.

2.3.3 Hanover potential

The Hanover group takes the Δ-isobar excitation into account to obtain an effective 3NP from any NNP. In this model, an explicit Δ-isobar is added to the nucleonic Hilbert space of a three-nucleon system [44]. The Δ-isobar is considered as a stable particle rather than a dynamic πN system and it is created in a two-nucleon scattering in a medium through the internal excitation of a nucleon [45]. The Δ-degree of freedom is treated in a coupled-channel approach. A two-baryon coupled-channel potential was developed which couples two-nucleon states to nucleon-Δ states. The transition potential from NN to NΔ states is derived from π- and ρ-exchange. The Coulomb interaction between protons in two-protons reactions has recently been included in the potential [46]. As a first step, the CD-Bonn+Δ potential was refitted to the Nijmegen data-base. This potential was then employed to describe elastic and inelastic 3N scattering [47]. This calculation has been performed only using the CD-Bonn potential until now, though it is planned to employ this method to other high-quality NNPs [48].

2.3.4 Effective Chiral Lagrangian approach

One believes that QCD will be able to describe the nuclear potential. However, in the energy range of interest in nuclear physics this has not been feasible yet, because the problem is non-perturbative. On the other hand, using the basic symmetries of QCD, one can construct a field theory of nucleons and pions with which nuclear physics phenomena could be explained. Based on the chiral symmetry of QCD,

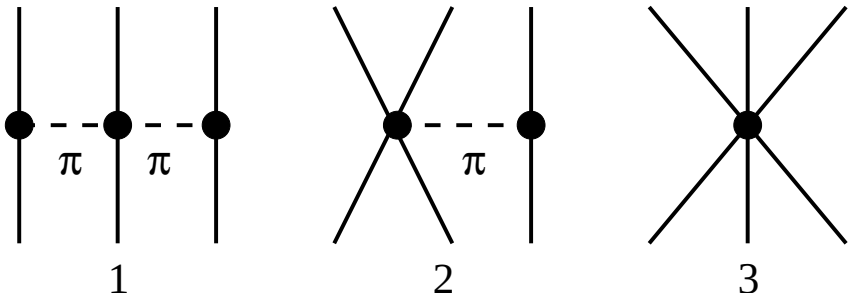

Figure 2.6: 3NP terms appearing in NNLO in χPT: 1) TPE, 2) OPE with the pion emitted or absorbed by NN contact interactions, and 3) 3N contact interaction.

Weinberg suggested a method [5, 6] by which the potential among any number of low-energy nucleons is expanded in powers of the nucleon momenta, Q/Λ, and the pion mass, m_π/Λ, scaled by a characteristic mass, Λ, of order of 1 GeV [49]. The highest momentum allowed for any involved particle is $Q \ll \Lambda$ and the nucleons with momenta greater than Q are integrated out. The lowest-order or the leading order (LO), Q^0/Λ^0, consists of OPEP and s-wave direct contact term and provides the longest range force between two nucleons. The next-to-leading order (NLO) potential consists of TPEP and higher partial waves such as p-wave direct two-nucleon contact interaction; and so on. The three-nucleon effective potential appears for the first time in the order of $(Q/\Lambda)^3$ or next-to-next-to-leading (NNLO). Figure 2.6 shows 3N vertices which make a contribution to the chiral 3NP in NNLO. The contribution of the diagrams in Fig. 2.6 was calculated in Refs. [40, 49]. Weinberg further showed the intuitive hierarchy of the few-nucleon forces: the NNP is more important than the 3NP, the 3NP is larger than the 4NP, and so on. Weinberg's proposal has been successful in the NN system [50, 51, 52, 53, 54], and is being studied in 3N scattering [55]. There are a few free parameters in the effective potential called the low-energy constants, coming from the effective Lagrangian, which have to be fitted to the πN data. It was shown later that the form of the derived effective 3NP matches the form of the existing phenomenological 3NPs, Eq. 2.49, as discussed extensively in Ref. [43].

2.3.5 Other 3NPs

There are other 3NPs on the market such as the Brazil 3NP. The Brazilian group derived a TPE 3NP using an effective Lagrangian [56]. They consider the s-wave and p-wave potentials and their relative importance. The 3NP of the Brazilian model in momentum space is quite similar to the TM potential, Eq. 2.49. A comparison

	$\mu a'$	$\mu^3 b$	$\mu^3 c$	$\mu^3 d$
FM[†]	0.0	–1.15	0.0	–0.29
TM[†]	–1.03	–2.62	1.03	–0.60
TM′[‡]	–1.12	–2.80	0.0	–0.75
Brazil[†]	–1.05	–2.29	1.05	–0.77
UIX[†]	0.0	–1.20	0.0	–0.30
Texas[†]	–1.87	–3.82	0.0	–1.12

[†]Ref. [43] and [‡]Ref. [38].

Table 2.1: Low-energy πN scattering parameters for some of the TPE 3NPs.

between the πN scattering parameters of various 3NPs of TPE-type is shown in Tab. 2.1.

2.4 The scattering observables

The most common observable in a scattering experiment is the cross section. In order to measure the cross section of a reaction, what we need is a beam of particles impinging on a target and a detector to observe the outgoing particles. In such a simple scattering experiment the cross section depends only on the polar angle, θ. If the beam of projectiles is polarized, then the cross section depends not only on the polar angle but also on the azimuthal angle, ϕ. This dependence can easily be observed by putting two detectors at the same polar angle but on the opposite sides of the beam. The ϕ-dependent part of the scattering cross section is characterized by the observable called analyzing power.

Having polarized incident particles, one can measure, in principal, many other polarization observables. For instance, the transfer of the polarization of the incoming particles to the outgoing particles. The coefficients that relate the polarization of the outgoing particles to that of the incoming ones are called the polarization-transfer coefficients. To measure the polarization of the outgoing particles, a second scattering is required, where by studying the asymmetry of the secondary scattering, one can measure the polarization of the secondary incident particles, namely the polarization of the outgoing particles of the primary reaction. These types of experiments are, therefore, called double-scattering experiments. The first scattering is usually the scattering process of interest and the second scattering is used to measure the polarization of the scattered particles.

Let us introduce first the concept of polarization for proton and deuteron beams. The concepts of polarization and experiments involving polarized beams and details

about the derivations can be found in Ref. [57]. The polarized source at KVI is an ion source, see Sec. 3.1. The polarized beam produced by an ion source has an axial symmetry because of the presence of a magnetic field in the source. It is convenient to take the axis of quantization along this magnetic field direction, Z axis. The X and Y axes are arbitrary because of the axial symmetry. This XYZ frame is called the *polarization frame* [57]. Polarized protons produced by the ion source have the states, $|j,m\rangle$, of spin-up, $|\frac{1}{2},\frac{1}{2}\rangle$, and spin-down, $|\frac{1}{2},-\frac{1}{2}\rangle$. If the populations of spin-up and spin-down in an ensemble are denoted by N_+ and N_-, respectively, the polarization of the ensemble is defined by:

$$p_Z = \frac{N_+ - N_-}{N_+ + N_-}. \tag{2.53}$$

Deuteron is a spin-1 particle, so it can be in three spin states, namely $|1,1\rangle$, $|1,0\rangle$ and $|1,-1\rangle$. If the populations of these states in an ensemble are denoted by N_+, N_0 and N_-, respectively, then a vector and a tensor polarization for such an ensemble in the polarization frame are defined as

$$\begin{aligned} p_Z &= \frac{N_+ - N_-}{N_+ + N_- + N_0}, \\ p_{ZZ} &= \frac{N_+ + N_- - 2N_0}{N_+ + N_- + N_0} = 1 - \frac{3N_0}{N_+ + N_- + N_0}. \end{aligned} \tag{2.54}$$

In the polarization frame, all other components vanish except p_{XX} and p_{YY} which, because of the axial symmetry, are related to p_{ZZ}:

$$p_{XX} = p_{YY} = -\frac{1}{2}p_{ZZ}. \tag{2.55}$$

Therefore, in the polarization coordinate system the vector polarization is $\vec{p} = (0,0,p_Z)$ and the tensor polarization is

$$\mathbf{P} = \begin{pmatrix} -\frac{1}{2}p_{ZZ} & 0 & 0 \\ 0 & -\frac{1}{2}p_{ZZ} & 0 \\ 0 & 0 & p_{ZZ} \end{pmatrix} = \frac{3}{2}p_{ZZ}\begin{pmatrix} 0&0&0 \\ 0&0&0 \\ 0&0&1 \end{pmatrix} - \frac{1}{2}p_{ZZ}\begin{pmatrix} 1&0&0 \\ 0&1&0 \\ 0&0&1 \end{pmatrix}.$$

The polarization frame is not the frame in which the measurements are performed. A frame that is generally used for a scattering reaction is the helicity frame, see Fig. 2.7. For projectile helicity frame, the $\hat{l}$ axis is defined parallel to particle momentum $\hat{k}_{in}$; the $\hat{n}$ axis is along the normal to the scattering plane, $\hat{n} = \frac{\vec{k}_{in}\times\vec{k}_{out}}{|\vec{k}_{in}\times\vec{k}_{out}|}$; and the $\hat{s}$ axis is defined in a way to make a right-handed coordinate system, $\hat{s} = \hat{n}\times\hat{l}$. In the figure, β is the angle between $\hat{k}_{in}$ and quantization axis $\hat{Z}$, and ϕ is the angle

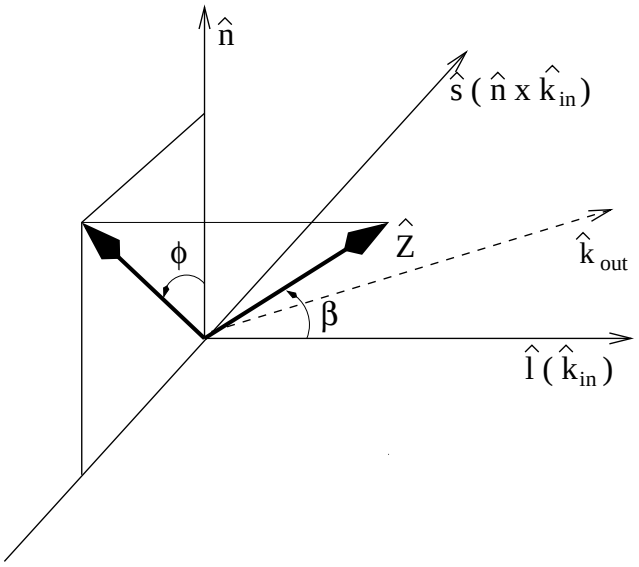

Figure 2.7: Beam polarization in the projectile helicity frame. $\hat{Z}$ is the natural quantization axis along the magnetic field and $\hat{n} = \hat{k}_{in} \times \hat{k}_{out}$ is normal to the scattering plane.

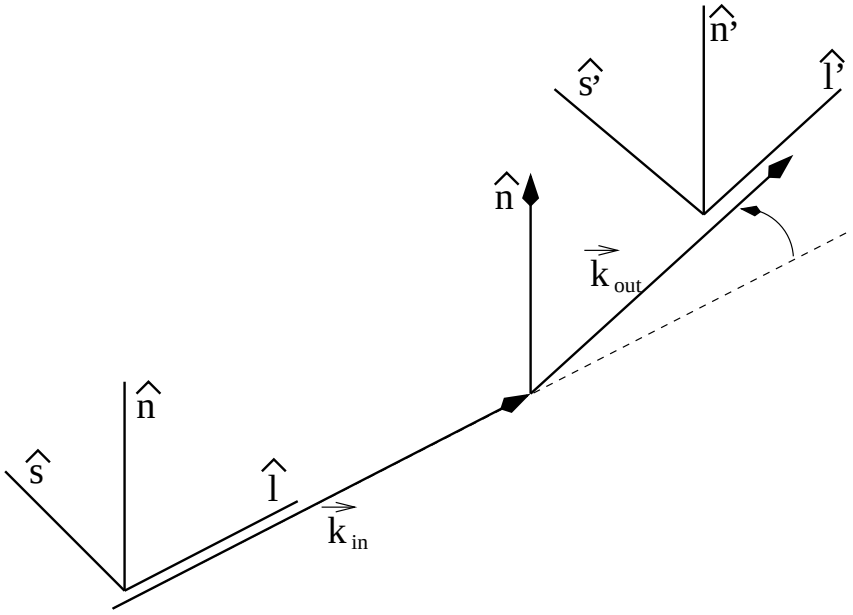

Figure 2.8: Projectile helicity frame (s, n, l) and outgoing helicity frame (s', n', l').

between $\hat{n}$ and the projection of $\hat{Z}$ in the $s-n$ plane. The transformation from polarization frame to helicity frame is performed via rotation operators. A rotation of β degrees around the s axis followed by a rotation of ϕ degrees around the l axis transforms the polarization to the projectile helicity frame. For vector polarization

$$\begin{aligned}\vec{p}_h = \begin{pmatrix} p_s \\ p_n \\ p_l \end{pmatrix} &= \begin{pmatrix} \cos\phi & -\sin\phi & 0 \\ \sin\phi & \cos\phi & 0 \\ 0 & 0 & 1 \end{pmatrix} \begin{pmatrix} 1 & 0 & 0 \\ 0 & \cos\beta & \sin\beta \\ 0 & -\sin\beta & \cos\beta \end{pmatrix} \begin{pmatrix} 0 \\ 0 \\ p_Z \end{pmatrix} \\ &= U \begin{pmatrix} 0 \\ 0 \\ p_Z \end{pmatrix} = \begin{pmatrix} -p_Z \sin\beta \sin\phi \\ p_Z \sin\beta \cos\phi \\ p_Z \cos\beta \end{pmatrix},\end{aligned} \tag{2.56}$$

where h denotes helicity and

$$U = \begin{pmatrix} \cos\phi & -\cos\beta\sin\phi & -\sin\beta\sin\phi \\ \sin\phi & \cos\beta\cos\phi & \sin\beta\cos\phi \\ 0 & -\sin\beta & \cos\beta \end{pmatrix}.$$

For the tensor polarization

$$\mathbf{P_h} = U\mathbf{P}U^t = \frac{3}{2}p_{ZZ}U \begin{pmatrix} 0 & 0 & 0 \\ 0 & 0 & 0 \\ 0 & 0 & 1 \end{pmatrix} U^t - \frac{1}{2}p_{ZZ} \begin{pmatrix} 1 & 0 & 0 \\ 0 & 1 & 0 \\ 0 & 0 & 1 \end{pmatrix}.$$

The non-zero components of the tensor polarization are:

$$\begin{aligned} p_{ss} &= \frac{1}{2}(3\sin^2\beta\ \sin^2\phi\ - 1)p_{ZZ}, \\ p_{nn} &= \frac{1}{2}(3\sin^2\beta\ \cos^2\phi\ - 1)p_{ZZ}, \\ p_{ll} &= \frac{1}{2}(3\cos^2\beta - 1)p_{ZZ}, \\ p_{sn} &= -\frac{3}{2}\sin^2\beta\ \cos\phi\ \sin\phi\ p_{ZZ}, \\ p_{nl} &= \frac{3}{2}\sin\beta\ \cos\beta\ \cos\phi\ p_{ZZ}, \\ p_{sl} &= -\frac{3}{2}\sin\beta\ \cos\beta\ \sin\phi\ p_{ZZ}. \end{aligned} \tag{2.57}$$

At present, only a beam polarization with $\beta = 90^\circ$ is available at KVI, so $p_{nl} = p_{sl} = 0$.

In the measurement of polarization-transfer coefficients, an outgoing helicity frame is also necessary. The $\hat{n}'$ axis for the outgoing helicity frame is parallel to $\hat{n}$. The $\hat{l}'$ axis is along $\hat{k}_{out}$ and $\hat{s}'$ completes the right-handed system; see Fig. 2.8.

There is a variety of spin-observables in the scattering process which can be studied. The form of the observables for the reactions studied in this thesis will be shown here. Suppose that the initial spin state of a scattering reaction is described by

$$\chi_i = \sum_j a_j \phi_j, \tag{2.58}$$

where ϕ_j makes the basis for spin states before the reaction, j is dimension of the space and i denotes "initial". The final state can be represented by

$$\chi_f = \sum_j b_j \phi'_j, \tag{2.59}$$

where ϕ'_j makes the basis for spin states after the reaction, and f denotes "final". The scattering amplitude, represented by M, relates the initial and final states:

$$\chi_f = M\chi_i \qquad \text{and} \qquad b_j = \sum_k M_{jk} a_k. \tag{2.60}$$

The initial and final density matrices are defined for an ensemble of N particles as

$$\rho_i \equiv \sum_{n=1}^{N} \chi_i^{(n)} [\chi_i^{(n)}]^\dagger \tag{2.61}$$

and

$$\rho_f \equiv \sum_{n=1}^{N} \chi_f^{(n)} [\chi_f^{(n)}]^\dagger. \tag{2.62}$$

By substituting Eq. 2.60 into Eq. 2.62 we obtain

$$\rho_f = M\rho_i M^\dagger. \tag{2.63}$$

If ρ_i is normalized to unity, the differential cross section for a polarized beam is given by

$$I(\theta, \phi) = Tr\rho_f = TrM\rho_i M^\dagger. \tag{2.64}$$

Observables of the $\mathbf{H}(\vec{p}, \vec{p})p$ reaction

The reaction $\mathrm{H}(\vec{p}, \vec{p})p$ was used in the calibration of the BBS polarimeter. The spin structure of the $\mathrm{H}(\vec{p}, \vec{p})p$ reaction is $\frac{\vec{1}}{2} + A \longrightarrow \frac{\vec{1}}{2} + B$. As a simple case, one can consider A and B to be spinless. All arguments will remain the same for the interesting case of non-zero spin for A and B. For the case of $\frac{\vec{1}}{2} + 0 \longrightarrow \frac{\vec{1}}{2} + 0$, one

can expand the density matrix in terms of the set of Pauli matrices, $\sigma_1, \sigma_2, \sigma_3$, and the unit matrix I:

$$\rho_i = \frac{1}{2}\left(I + \sum_{j=1}^{3} p_j \sigma_j\right). \tag{2.65}$$

For any operator Ω, We have $\langle\Omega\rangle = Tr\rho_i\Omega$. Therefore:

$$p_j \equiv \langle\sigma_j\rangle = Tr\rho_i\sigma_j \tag{2.66}$$

is the j^{th} component of the beam polarization. By substituting Eq. 2.65 into 2.64 we obtain

$$I(\theta,\phi) = I_0(\theta)\left(1 + \sum_{j=1}^{3} p_j A_j(\theta)\right), \tag{2.67}$$

where

$$A_j(\theta) \equiv \frac{TrM\sigma_j M^\dagger}{TrMM^\dagger} \tag{2.68}$$

is the j^{th} component of the analyzing power, and

$$I_0(\theta) = \frac{1}{2} TrMM^\dagger \tag{2.69}$$

is the cross section for an unpolarized beam. Similarly, the polarization of the outgoing particles can be calculated through

$$p_{k'} I(\theta,\phi) = I_0(\theta)\left(P_{k'}(\theta) + \sum_{j=1}^{3} p_j K_j^{k'}(\theta)\right), \tag{2.70}$$

where

$$P_{k'}(\theta) = \frac{TrMM^\dagger\sigma_{k'}}{TrMM^\dagger} \tag{2.71}$$

is the k'^{th} component of polarization which is produced by an unpolarized beam and is called the induced polarization. Time-reversal invariance implies that $\overline{P_n} = A_n$ where the bar refers to time-reversed reaction. For an elastic scattering where the forward and reverse reactions are the same $P_n = A_n$. The polarization-transfer coefficient $K_j^{k'}(\theta)$ from the j^{th} initial polarization component to k'^{th} final polarization component is given by

$$K_j^{k'}(\theta) = \frac{TrM\sigma_j M^\dagger\sigma_{k'}}{TrMM^\dagger}. \tag{2.72}$$

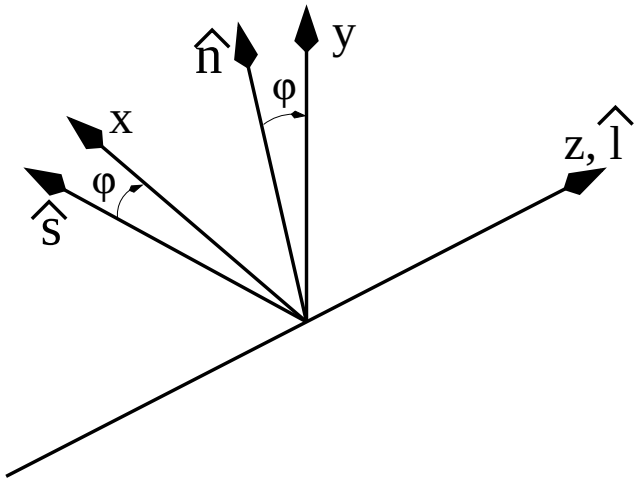

Figure 2.9: The relation between the incoming helicity frame and the laboratory frame.

For a general parity-conserving reaction with $A(\vec{\frac{1}{2}}, \vec{\frac{1}{2}})B$ spin structure, the cross section and polarization can be written as

$$\begin{aligned} I &= I_0\,(1 + p_n A_n(\theta))\,, \\ p_{s'} I &= I_0(p_s K_s^{s'}(\theta) + p_l K_l^{s'}(\theta)), \\ p_{n'} I &= I_0(P_{n'}(\theta) + p_n K_n^{n'}(\theta)), \\ p_{l'} I &= I_0(p_s K_s^{l'}(\theta) + p_l K_l^{l'}(\theta)). \end{aligned} \tag{2.73}$$

All other coefficients are zero. To use Eq. 2.73, one must transform it from the helicity frame into the laboratory coordinate system. Figure 2.9 shows the relation between the incoming helicity frame and the laboratory frame. One can easily write the unit vector of the incoming helicity frame in the laboratory frame. In matrix form, these relations are

$$\hat{l} = \begin{pmatrix} 0 \\ 0 \\ 1 \end{pmatrix}, \quad \hat{n} = \begin{pmatrix} \sin\phi \\ \cos\phi \\ 0 \end{pmatrix} \text{ and } \quad \hat{s} = \begin{pmatrix} \cos\phi \\ -\sin\phi \\ 0 \end{pmatrix}, \tag{2.74}$$

where ϕ is shown in Fig. 2.9. A rotation of θ degrees around the $\hat{n}$ axis transforms the incoming helicity frame into outgoing helicity frame. Therefore,

$$\hat{l'} = \begin{pmatrix} \sin\theta\cos\phi \\ -\sin\theta\sin\phi \\ \cos\theta \end{pmatrix}, \quad \hat{n'} = \begin{pmatrix} \sin\phi \\ \cos\phi \\ 0 \end{pmatrix} \text{ and } \quad \hat{s'} = \begin{pmatrix} \cos\theta\cos\phi \\ -\cos\theta\sin\phi \\ -\sin\theta \end{pmatrix} \tag{2.75}$$

are the unit vectors of the outgoing helicity frame in the laboratory frame. Let $\vec{p'}$ be the outgoing polarization in the laboratory frame. Using Eq. 2.75 and the fact that one can write $\vec{p'} = p_{s'}\hat{s'} + p_{n'}\hat{n'} + p_{l'}\hat{l'}$, the components of $\vec{p'}$ are

$$\vec{p'} = \begin{pmatrix} p_{x'} \\ p_{y'} \\ p_{z'} \end{pmatrix} = \frac{I_0}{I} \begin{pmatrix} p_{s'}\cos\theta\cos\phi + p_{n'}\sin\phi + p_{l'}\sin\theta\cos\phi \\ -p_{s'}\cos\theta\sin\phi + p_{n'}\cos\phi - p_{l'}\sin\theta\sin\phi \\ -p_{s'}\sin\theta + p_{l'}\cos\theta \end{pmatrix}. \tag{2.76}$$

To obtain the relation between the incoming and outgoing polarizations in the laboratory frame, one must substitute the $p_{s'}, p_{n'}$ and $p_{l'}$ components in terms of the polarization of the incoming particles in the laboratory frame, p_x, p_y and p_z. If the polarization of the incoming beam in the laboratory frame is assumed to be

$$\vec{p} = \begin{pmatrix} p_x \\ p_y \\ p_z \end{pmatrix},$$

then the polarization in projectile helicity frame is

$$\vec{p}_{ih} = \begin{pmatrix} p_s \\ p_n \\ p_l \end{pmatrix} = \begin{pmatrix} \cos\phi & -\sin\phi & 0 \\ \sin\phi & \cos\phi & 0 \\ 0 & 0 & 1 \end{pmatrix} \begin{pmatrix} p_x \\ p_y \\ p_z \end{pmatrix} = \begin{pmatrix} p_x\cos\phi - p_y\sin\phi \\ p_x\sin\phi + p_y\cos\phi \\ p_z \end{pmatrix}, \tag{2.77}$$

where i denotes "initial" and h the "helicity". A polarized beam accelerated by a cyclotron is assumed to have no x and z components, though analysis of the polarized beam produced at KVI shows a small p_x polarization; see Sec. 4.1.1. Therefore, only the p_z component in Eq. 2.77 will be set to zero. The relation between polarization of the incoming particles and that of outgoing particles in helicity frame is given by Eq. 2.73. In matrix form, Eq. 2.73 can be written as

$$\vec{p}_{fh} = \begin{pmatrix} p_{s'} \\ p_{n'} \\ p_{l'} \end{pmatrix} = \frac{I_0}{I} \begin{pmatrix} 0 \\ P_n \\ 0 \end{pmatrix} + \frac{I_0}{I} \begin{pmatrix} K_s^{s'} & 0 & K_l^{s'} \\ 0 & K_n^{n'} & 0 \\ K_s^{l'} & 0 & K_l^{l'} \end{pmatrix} \begin{pmatrix} p_s \\ p_n \\ p_l \end{pmatrix}$$

$$= \frac{I_0}{I} \begin{pmatrix} p_s K_s^{s'} + p_l K_l^{s'} \\ P_n + p_n K_n^{n'} \\ p_s K_s^{l'} + p_l K_l^{l'} \end{pmatrix} = \frac{I_0}{I} \begin{pmatrix} (p_x\cos\phi - p_y\sin\phi)K_s^{s'} \\ P_n + (p_x\sin\phi + p_y\cos\phi)K_n^{n'} \\ (p_x\cos\phi - p_y\sin\phi)K_s^{l'} \end{pmatrix}, \tag{2.78}$$

where f denotes "final" and

$$\frac{I_0(\theta)}{I(\theta,\phi)} = \frac{1}{1 + p_n A_n} = \frac{1}{1 + (p_x\sin\phi + p_y\cos\phi)A_n}. \tag{2.79}$$

To obtain the relation between the incoming and outgoing polarizations in laboratory frame, all we need to do is to substitute Eq. 2.78 into Eq. 2.76. The analyzing power A_n, induced polarization P_n and polarization transfer coefficients $K_s^{s'}$, $K_n^{n'}$ and $K_s^{l'}$ have been obtained from the Nijmegen data-base with a PWA [58].

Observables of the H$(\vec{d},\vec{p})d$ reaction

The spin structure of the H$(\vec{d},\vec{p})d$ reaction is $\vec{1}+A \longrightarrow \vec{\frac{1}{2}}+B$. The same procedure as for the H$(\vec{p},\vec{p})p$ reaction leads us to the following equations:

$$I(\theta,\phi) = I_0(\theta)\left(1+\frac{3}{2}\sum_j p_j A_j(\theta)+\frac{1}{3}\sum_{j,k} p_{jk}A_{jk}\right), \tag{2.80}$$

$$p_{i'}I(\theta,\phi) = I_0(\theta)\left(P_{i'}(\theta)+\frac{3}{2}\sum_j p_j K_j^{i'}+\frac{1}{3}\sum_{j,k} p_{jk}K_{jk}^{i'}\right), \tag{2.81}$$

where p_j is the vector component and p_{jk} the tensor component of the beam polarization and

$$A_j(\theta) = \frac{TrMP_jM^\dagger}{TrMM^\dagger} \quad \text{vector analyzing powers,} \tag{2.82}$$

$$A_{jk}(\theta) = \frac{TrMP_{jk}M^\dagger}{TrMM^\dagger} \quad \text{tensor analyzing powers,} \tag{2.83}$$

$$P_{i'}(\theta) = \frac{TrMM^\dagger\sigma_{i'}}{TrMM^\dagger} \quad \text{induced polarization,} \tag{2.84}$$

$$K_j^{i'}(\theta) = \frac{TrMP_jM^\dagger\sigma_{i'}}{TrMM^\dagger} \quad \text{vector polarization-transfer coefficients,} \tag{2.85}$$

$$K_{jk}^{i'}(\theta) = \frac{TrMP_{jk}M^\dagger\sigma_{i'}}{TrMM^\dagger} \quad \text{tensor polarization-transfer coefficients.} \tag{2.86}$$

Here, P_j and P_{jk} are a complete set of operators which makes a basis for the spin space of spin-1 particles. Parity conservation eliminates many of the terms in Eq. 2.80 and 2.81. Thus, for the elastic scattering of a polarized deuteron beam

from an unpolarized hydrogen target we have

$$\begin{aligned}
I &= I_0\left(1+\frac{3}{2}p_nA_n+\frac{2}{3}p_{sl}A_{sl}+\frac{1}{3}(p_{ss}A_{ss}+p_{nn}A_{nn}+p_{ll}A_{ll})\right),\\
p_{s'}I &= I_0\left(\frac{3}{2}(p_sK_s^{s'}+p_lK_l^{s'})+\frac{2}{3}(p_{sn}K_{sn}^{s'}+p_{nl}K_{nl}^{s'})\right),\\
p_{n'}I &= I_0\left(P_{n'}+\frac{3}{2}p_nK_n^{n'}+\frac{2}{3}p_{sl}K_{sl}^{n'}+\frac{1}{3}(p_{ss}K_{ss}^{n'}+p_{nn}K_{nn}^{n'}+p_{ll}K_{ll}^{n'})\right),\\
p_{l'}I &= I_0\left(\frac{3}{2}(p_sK_s^{l'}+p_lK_l^{l'})+\frac{2}{3}(p_{sn}K_{sn}^{l'}+p_{nl}K_{nl}^{l'})\right).
\end{aligned} \tag{2.87}$$

To use Eq. 2.87, the polarizations on the right side of the equation must be substituted by Eq. 2.56 and Eq. 2.57. The relation between the polarization of the scattered particles in the helicity and laboratory frames in the left side of Eq. 2.87 is

$$p_{y'}=\frac{p_{n'}}{\cos\phi}, \tag{2.88}$$

where ϕ is the azimuthal angle of scattering. There are a few identities which might be used to change the form of Eq. 2.87. The tensor components of the polarization satisfy the identity

$$p_{ss}+p_{nn}+p_{ll}=0. \tag{2.89}$$

Also, the tensor analyzing powers and the polarization-transfer coefficients satisfy similar identities

$$A_{ss}+A_{nn}+A_{ll}=0, \tag{2.90}$$

$$K_{ss}^{n'}+K_{nn}^{n'}+K_{ll}^{n'}=0. \tag{2.91}$$

Using these identities, one can obtain two other useful identities

$$\frac{1}{3}(p_{ss}A_{ss}+p_{nn}A_{nn}+p_{ll}A_{ll})=\frac{1}{6}(p_{tt}-p_{mm})(A_{tt}-A_{mm})+\frac{1}{2}p_{kk}A_{kk}, \tag{2.92}$$

$$\frac{1}{3}(p_{ss}K_{ss}^{n'}+p_{nn}K_{nn}^{n'}+p_{ll}K_{ll}^{n'})=\frac{1}{6}(p_{tt}-p_{mm})(K_{tt}^{n'}-K_{mm}^{n'})+\frac{1}{2}p_{kk}K_{kk}^{n'}, \tag{2.93}$$

where t,m,k are s,n,l in any order. The identities 2.92 and 2.93 can be used to rewrite Eq. 2.87 in a form which might be more convenient for a specific experiment. In the following, the convenient form of Eq. 2.87 for the present $\mathrm{H}(\vec{d},\vec{p})d$ reaction will be obtained. The vector and tensor polarizations (p_Z and p_{ZZ} in Eq. 2.54) can be measured by the In-Beam Polarimeter (IBP); see Sec. 4.1. By inserting p_Z and

p_{ZZ} in Eq. 2.56 and 2.57 and setting $\beta = 90°$, the non-zero components can be obtained:

$$\vec{p}_h = \begin{pmatrix} p_s \\ p_n \\ p_l \end{pmatrix} = \begin{pmatrix} -p_Z \sin\phi \\ p_Z \cos\phi \\ 0 \end{pmatrix}, \tag{2.94}$$

and

$$\begin{aligned} p_{ss} &= \frac{1}{2}(3\sin^2\phi\ -1)p_{ZZ}, \\ p_{nn} &= \frac{1}{2}(3\cos^2\phi\ -1)p_{ZZ}, \\ p_{ll} &= -\frac{1}{2}p_{ZZ}, \\ p_{sn} &= -\frac{3}{2}\cos\phi\ \sin\phi\ p_{ZZ}, \\ p_{ss} - p_{ll} &= \frac{3}{2}\sin^2\phi\ p_{ZZ}, \\ p_{sl} &= p_{nl} = 0. \end{aligned} \tag{2.95}$$

Therefore, Eq. 2.87 can be rewritten as:

$$\begin{aligned} I &= I_0\left(1 + \frac{3}{2}p_Z\cos\phi A_n + \frac{1}{4}\sin^2\phi\ p_{ZZ}(A_{ss} - A_{ll}) + \frac{1}{4}(3\cos^2\phi - 1)p_{ZZ}A_{nn}\right), \\ p_{s'}I &= I_0\left(-\frac{3}{2}p_Z K_s^{s'} - \cos\phi\ p_{ZZ}K_{sn}^{s'}\right)\sin\phi, \\ p_{n'}I &= I_0\left(P_{n'} + \frac{3}{2}p_Z\cos\phi K_n^{n'} + \frac{1}{4}\sin^2\phi\ p_{ZZ}(K_{ss}^{n'} - K_{ll}^{n'}) + \frac{1}{4}(3\cos^2\phi - 1)p_{ZZ}K_{nn}^{n'}\right), \\ p_{l'}I &= I_0\left(-\frac{3}{2}p_Z K_s^{l'} - \cos\phi\ p_{ZZ}K_{sn}^{l'}\right)\sin\phi. \end{aligned} \tag{2.96}$$

The employed detector for the experiment has an aperture with $\phi = 180° \pm \phi_m$ where ϕ_m varies between 5° to 15° depending on the position of the detector. Integration over ϕ distribution of the events will cancel out the terms with $\sin\phi$ and $\sin^2\phi$. Therefore, the remaining terms of Eq. 2.96 are:

$$\begin{aligned} I &= I_0\left(1 + \frac{3}{2}p_Z\cos\phi A_n + \frac{1}{4}(3\cos^2\phi - 1)p_{ZZ}A_{nn}\right), \\ p_{n'}I &= I_0\left(P_{n'} + \frac{3}{2}p_Z\cos\phi K_n^{n'} + \frac{1}{4}(3\cos^2\phi - 1)p_{ZZ}K_{nn}^{n'}\right). \end{aligned} \tag{2.97}$$

In our experiment, I_0, $P_{n'}$, A_n, A_{nn}, $K_n^{n'}$ and $K_{nn}^{n'}$ have been measured for several center-of-mass angles.

Sometimes, spherical coordinates are used to derive the formulas. The relations between spherical and Cartesian analyzing powers are:

$$\begin{aligned} iT_{11} &\equiv \frac{\sqrt{3}}{2}A_n, \\ T_{20} &\equiv \frac{1}{\sqrt{2}}A_{ll}, \\ T_{21} &\equiv -\frac{1}{\sqrt{3}}A_{sl}, \\ T_{22} &\equiv \frac{1}{2\sqrt{3}}(A_{ss} - A_{nn}). \end{aligned} \tag{2.98}$$

Using these relations, the cross section of Eq. 2.96 can be written as:

$$I(\theta,\phi) = I_0(\theta)\left[1 + \sqrt{3}p_Z iT_{11}(\theta)\cos\phi - \frac{1}{\sqrt{8}}p_{ZZ}T_{20}(\theta) - \frac{\sqrt{3}}{2}p_{ZZ}T_{22}(\theta)\cos 2\phi\right]. \tag{2.99}$$

This form of cross section will be used for the analysis of the In-Beam Polarimeter data. In most of the literatures the helicity coordinates are indicated by (x, y, z) which corresponds to (s, n, l) in this chapter. In order to be consistent with literature the (x, y, z) coordinates are used for helicity frame in chapter 4.